



**Thermoresponsive Block Copolymer Micelles with Tunable
Pyrrolidone-based Polymer Cores: Structure/Property
Correlations and Application as Drug Carriers**

| | |
|-------------------------------|---|
| Journal: | <i>Journal of Materials Chemistry B</i> |
| Manuscript ID: | TB-ART-09-2014-001494.R1 |
| Article Type: | Paper |
| Date Submitted by the Author: | 29-Oct-2014 |
| Complete List of Authors: | Sun, Xiao-Li; Rutgers University - Newark, Chemistry Tsai, Pei-Chin; Rutgers University, Department of Pharmaceutics Bhat, Rajani; Rutgers University - Newark, Chemistry Bonder, Edward; Rutgers University - Newark, Department of Biological Sciences Michniak-Kohn, Bozena; Rutgers University, Department of Pharmaceutics Pietrangelo, Agostino; Rutgers University, Department of Chemistry |
| | |

ARTICLE

Thermoresponsive Block Copolymer Micelles with Tunable Pyrrolidone-based Polymer Cores: Structure/Property Correlations and Application as Drug Carriers†

Cite this: DOI: 10.1039/x0xx00000x

Received 00th January 2012,
Accepted 00th January 2012

DOI: 10.1039/x0xx00000x

www.rsc.org/

X.-L. Sun,^a P.-C. Tsai,^b R. Bhat,^a E. M. Bonder,^c B. Michniak-Kohn,^b and A. Pietrangelo^d

A-B Block copolymer micelles comprised of thermoresponsive hydrophilic PNIPAAm (poly(*N*-isopropylacrylamide)) coronae and hydrophobic PNP (poly(*N*-acryloyl-2-pyrrolidone)), PMNP (poly(*N*-acryloyl-5-methoxy-2-pyrrolidone)), or PBNP (poly(*N*-acryloyl-5-butoxy-2-pyrrolidone)) cores were examined to identify how systematic adjustments to core-segment structure affect micellar physicochemical properties, drug loading efficiency (DLE), and thermoresponsive drug release among these novel systems. Critical micelle concentrations (CMCs) were found to decrease by two orders of magnitude in the order of PNIPAAm-PNP, PNIPAAm-PMNP, and PNIPAAm-PBNP indicating that minor modifications to the pyrrolidone scaffold significantly affect its hydrophobic character. Moreover, the structural modifications were also found to influence micelle size and intermicellar aggregation that occurs above the lower critical solution temperature (LCST). In line with the CMC data, DLE values of doxorubicin-loaded (*i.e.*, DOX-loaded) micelles increase in the order of PNIPAAm-PNP, PNIPAAm-PMNP, and PNIPAAm-PBNP, a trend attributed to enhanced cohesive forces (*i.e.* London dispersion forces) between DOX and core as the latter becomes more hydrophobic. When heated above the LCST, DOX release decreases in the order of PNIPAAm-PNP, PNIPAAm-PMNP, and PNIPAAm-PBNP suggesting that release processes are impeded by the cohesive forces responsible for efficient encapsulation. Finally, cytotoxicity assays performed above the LCST reveal that DOX-loaded micelles are as cytotoxic as the free drug in formulations where DOX concentrations are equivalent.

Introduction

Block copolymer micelles are studied extensively for their encapsulating abilities that are attractive for nanoscale drug-delivery applications.^{1,2,3,4} Comprised of hydrophobic and hydrophilic segments, block copolymers can spontaneously self-assemble into core-shell architectures that provide a hydrophobic solubilizing microenvironment for lipophilic pharmaceuticals that are otherwise poorly soluble in aqueous media. As colloidal aggregates, the micellar scaffolds also shield therapeutic drugs from unwanted interactions with healthy tissues^{5,6,7} and increase blood residence times by reducing the rate of body clearance facilitated by the reticuloendothelial system.^{8,9,10} Moreover, the chemical flexibility of the block copolymer permits: 1) customization of the hydrophobic interior to improve drug-loading capacity¹¹ and 2) surface modification to the hydrophilic exterior to enhance target efficiency and specificity of tissue targeting.^{12,13}

Currently, there is interest in preparing *smart* micellar drug-delivery vehicles that expel pharmaceuticals in both a spatially and temporally controlled manner upon application of external stimuli such as pH^{14,15,16}, magnetic field,^{17,18} or temperature.^{19,20,21} The latter is particularly appealing since the application of heat to an affected area is both convenient and toxicologically safe.²² To impart this mode of activation, many micellar models employ poly(*N*-isopropylacrylamide) (PNIPAAm) as the hydrophilic thermosensitive block that undergoes a phase transition upon exceeding its LCST.²³ During this phase transition, the PNIPAAm blocks become hydrophobic resulting in collapse of the micellar corona, increased intermicellar aggregation, and expulsion of drug from the hydrophobic cores (Fig. 1).^{24,25,26,27,28,29,30,31,32,33,34}

While the thermoresponsivity of a micelle arises from the hydrophilic PNIPAAm corona, its drug-loading capacity is a direct consequence of noncovalent interactions between the hydrophobic core and lipophilic drug. Encapsulation is a complex phenomenon that relies on multiple related mechanisms such as the hydrophobic effect,^{35,36} polymer/drug

miscibility,^{37,38} electrostatic complexation,^{39,40} and/or secondary interactions such as π - π stacking^{41,42} or hydrogen-bonding.⁴³ To date, few experimental studies have examined drug loading and thermoresponsive release profiles as a function of block copolymer structure. Moreover, in past reports, micelles were comprised of hydrophobic repeat units with exceedingly diverse chemical architectures (e.g., poly(styrene) vs. poly(butyl methacrylate),⁴⁴ or, poly(lactide) vs. poly(ϵ -caprolactone)²²), hence structure/property correlations cannot be adequately addressed. As such, there remains a need for comparative analyses that evaluate thermoresponsive block copolymer micelles with only modest differences in their hydrophobic interior in order to assess the influence that core-structure has on drug loading and release phenomena, information that is critical to establishing design criteria for micellar drug delivery vehicles with efficient encapsulation and release profiles.

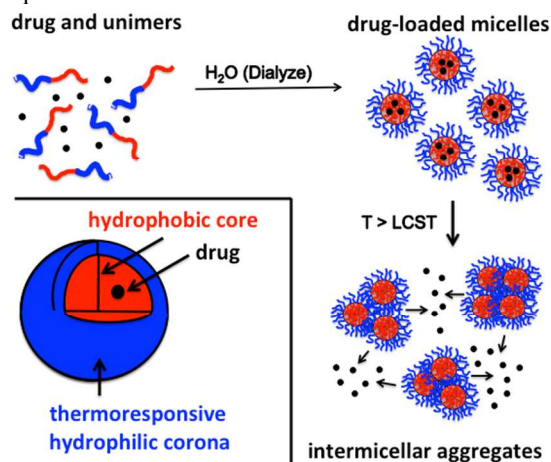


Fig. 1 Release mechanism for lipophilic drug delivery using thermoresponsive block copolymer micelles.

Inspired by the extensive use of poly(*N*-vinylpyrrolidone) as a multifunctional material in the pharmaceutical, cosmetic, textile, and food industries,^{45,46,47} we recently reported on the synthesis of novel functionalized pyrrolidone-based (co)polymers prepared from pyroglutamic acid, a bio-derived resource.⁴⁸ This work describes a convenient route to alkoxy-functionalized *N*-acryloyl-2-pyrrolidones that subsequently afford (co)polymers with tunable physicochemical properties that are conveniently manipulated through modest adjustments to alkoxy residue structure (e.g. methoxy, ethoxy, butoxy, and methoxy ethoxy). In light of these results, block copolymer micelles with thermoresponsive PNIPAAm coronae and poly(*N*-acryloyl-2-pyrrolidone) cores were considered attractive candidates for our studies given the structural tunability of the pyrrolidone scaffold and the biocompatibility and coordination ability that it lends to polymers of similar structure.^{49,50,51,52,53,54,55,56,57} To this end, block copolymer self-assembly, intermicellar aggregation, drug loading efficiency (DLE), and thermoresponsive drug release were examined using three sets of block copolymers that are distinguishable only by the pyrrolidone moiety (i.e., 2-pyrrolidone, 5-methoxy-2-pyrrolidone, and 5-butoxy-2-pyrrolidone) or hydrophobic block length. The performance of these systems as drug carriers was evaluated using the anthracycline chemotherapeutic agent doxorubicin⁵⁸ as the hydrophobic payload and MCF-7 breast cancer cells as the biological target. Ultimately, this work sets out to identify how both the addition and lengthening of simple

aliphatic alkoxy residues (i.e., MeO and BuO) tethered to the pyrrolidone moieties influence the physicochemical properties of the block copolymer micelles and their ability to serve as thermoresponsive drug carriers.

Experimental

Materials and Equipment. All polymerizations were performed in an inert atmosphere. Azobis(isobutyronitrile) (AIBN) was purchased from Aldrich and recrystallized from methanol prior to use. *N*-isopropylacrylamide (NIPAAm) was purchased from VWR and twice recrystallized from benzene/hexanes (65/35 v/v) prior to use. THF was dried and collected from a PureSolv MD solvent purification system (Innovative Technology Inc.) equipped with two activated alumina columns. All other solvents and reagents were used as received. Benzyl dithiobenzoate,^{59,60} *N*-acryloyl-5-methoxy-2-pyrrolidone (MNP), and *N*-acryloyl-5-butoxy-2-pyrrolidone (BNP)⁴⁸ were prepared according to literature procedures. ¹H NMR spectra were recorded on a Varian INOVA 500 spectrometer and calibrated to the residual protonated solvent peak at $\delta = 7.24$ for deuterated chloroform (CDCl₃). UV/vis spectra were recorded on a Cary-100 spectrophotometer equipped with a peltier heated multi-cell holder and Cary temperature controller and probe. Excitation and emission spectra were measured on a Varian Cary Eclipse fluorescence spectrophotometer. GPC analyses were performed in DMF/0.01 M LiBr (0.5 mL/min) using a Waters Empower system equipped with a 717plus autosampler, a 1525 binary HPLC pump, a 2487 dual λ absorbance detector, and a 2414 refractive index detector. Two styragel columns (Polymer Laboratories; 5 μ m Mix-C, column heater, 50 °C) were used for separation. Molecular weights were determined from a 12-point calibration curve using poly(methyl methacrylate) standards. Dynamic light scattering (DLS) measurements were performed on a Malvern Zetasizer Nano-ZS instrument, equipped with a 4 mW, 633 nm HeNe laser and an Avalanche photodiode detector at an angle of 173°. Transmission electron microscopy (TEM) was conducted on a FEI Tecnai 12 electron microscope operated at 80 kV. Samples were prepared by placing a drop of polymer micelle solution onto carbon coated copper grids followed by staining with an aqueous uranyl acetate solution (1% w/w).

Synthesis of *N*-acryloyl-2-pyrrolidone (NP). NP was prepared according to reported methods^{61,62} with the following modifications. Under a nitrogen atmosphere, *n*-butyllithium in hexanes (1.6 M, 25 mmol, 15.6 mL) was added dropwise over a period of 40 min to a solution of 2-pyrrolidone (25 mmol, 1.9 mL) in dry THF (ca. 70 mL) at -78°C. After 1 h of stirring, acryloyl chloride (30 mmol, 2.4 mL) was added dropwise followed by 5 h of additional stirring at -78°C. The reaction was quenched with saturated aqueous NH₄Cl (ca. 5 mL) and warmed to room temperature. A drop of *tert*-butyl catechol solution (15 mM, acetone) was added to the reaction mixture and the solvent removed by reduced pressure. The residue was taken up in ethyl acetate (ca. 20 mL) and water (ca. 10 mL) and the mixture extracted with ethyl acetate (3 x 30 mL). The combined organic phases were washed with saturated NaHCO₃ (ca. 10 mL) and brine (ca. 10 mL), and dried over anhydrous MgSO₄. After filtering the mixture, an additional drop of inhibitor (*tert*-butyl catechol solution) was added to the filtrate and the solvent removed under reduced pressure to afford a yellow oil. The crude product was purified by column chromatography (silica, ethyl acetate/hexanes, 1:1 v/v, R_f =

0.50). ^1H NMR (CDCl_3 , 500 MHz): δ 7.44 (1H, dd, $^3J_{\text{HH}} = 17.05$ Hz, $^3J_{\text{HH}} = 10.47$ Hz), 6.47 (1H, dd, $^3J_{\text{HH}} = 17.05$ Hz, $^3J_{\text{HH}} = 1.90$ Hz), 5.81 (1H, dd, $^3J_{\text{HH}} = 10.47$ Hz, $^3J_{\text{HH}} = 1.90$ Hz), 3.84 (2H, t, $^3J_{\text{HH}} = 7.18$ Hz), 2.60 (2H, t, 8.04), 2.04 (2H, m). ^{13}C NMR (CDCl_3 , 100 MHz): δ 175.6, 166.0, 130.8, 129.1, 45.6, 33.8, 17.2.

Synthesis of PNIPAAm-CTA. A pressure vessel (equipped with a sidearm and stir bar) was charged with *N*-isopropylacrylamide (11.3g, 0.1 mol), benzyl dithiobenzoate (136 mg, 0.56 mmol), AIBN (18 mg, 0.11mmol), and THF (*ca.* 12 mL). The solution was degassed using freeze-pump-thaw techniques (3 cycles) and immersed in a preheated oil bath at 80°C for 16 hours. The reaction was quenched by cooling the solution in a liquid nitrogen bath followed by precipitation in diethyl ether. The polymer was isolated by filtration and dried under vacuum to afford a pink solid (4.28 g, 38% yield). $M_n^{\text{NMR}} = 8380$, $M_n^{\text{GPC}} = 7600$, $M_w/M_n = 1.15$. A degree of polymerization (DP_n) of 72 was calculated by end-group analysis using ^1H NMR spectroscopy (Supplementary Information, Fig. S1).

Synthesis of Block Copolymers. All block copolymers were synthesized using PNIPAAm-CTA as the macromolecular chain-transfer agent and AIBN as the initiator. All block copolymers were prepared in THF with the exceptions of PNIPAAm₇₂-PNP₇₉ and PNIPAAm₇₂-PNP₂₉ that were prepared in anhydrous dimethylformamide (DMF). The feed ratios of PNIPAAm-CTA:(B,M)NP were adjusted to achieve different chain lengths of the P(B,M)NP block. In general, a pressure vessel was charged with solvent (*ca.* 1.5 mL), monomer, PNIPAAm-CTA (*ca.* 200 mg), and AIBN using the following molar ratios: 1) 45:1:0.2 (PNIPAAm₇₂-PBNP₂₆), 2) 95:1:0.2 (PNIPAAm₇₂-PBNP₇₃), 3) 45:1:0.2 (PNIPAAm₇₂-PMNP₂₉), 4) 95:1:0.2 (PNIPAAm₇₂-PMNP₇₈), 5) 30:1:0.2 (PNIPAAm₇₂-PNP₂₉), and 6) 90:1:0.2 (PNIPAAm₇₂-PNP₇₉). The solution was degassed using freeze-pump-thaw techniques (3 cycles) and immersed in a preheated oil bath at 80°C for *ca.* 2 hours. The reaction was quenched by cooling the solution in a liquid nitrogen bath followed by precipitation in diethyl ether. The polymer was isolated by filtration and dried under vacuum to afford a pink solid.

Preparation of Block Copolymer Micelles. In a typical experiment, 1 mL of block copolymer solution (2 mg/mL, DMF) was added to 8 mL of deionized water under vigorous stirring at a rate of 0.1 mL/min. The mixture was then placed in a dialysis bag (MWCO = 3.5 kDa) and dialyzed against deionized water for 48 h.

Fluorescence Measurements for CMC Determination. CMC data were collected according to literature procedures.⁶³ Aliquots (*ca.* 1 mL) of a pyrene stock solution (3.0×10^{-6} M in acetone) were dispensed into vials and stored in the absence of light until the solvent completely evaporated. Aliquots (*ca.* 5 mL) of aqueous micelle solutions over a broad concentration range were added to vials and stored at room temperature for 24 h. The excitation spectra of these solutions were recorded between 250 and 360 nm at $\lambda_{\text{em}} = 390$ nm. The intensity ratio (I_{337}/I_{334}) of the bands at 337 nm and 334 nm were plotted as a function of block copolymer concentration using a logarithmic scale. CMC values were determined as the point of intersection between two logarithmic lines of regression generated by KaleidaGraph software.

Preparation of DOX-Loaded Block Copolymer Micelles. Block copolymer (*ca.* 10 mg) was added to a solution of DOX-HCl (*ca.* 5 mg, 0.009 mmol), triethylamine (18 μL , 0.13 mmol) and *N*-ethylacetamide (*ca.* 5 mL) and stirred at room temperature for 12 h. The solution was added to 20 mL of deionized water at a rate of 0.1 mL/min and stirred for an additional 24 h. The solution was transferred to a dialysis bag (MWCO = 14-16 kDa) and dialyzed against deionized water (*ca.* 300 mL) for 20 h (using a fresh dialysis bag and water after 10 h). The amount of DOX loaded into the micelles was determined by fluorescence spectroscopy. During the dialysis procedure, an aliquot (100 μL) of the micelle solution was removed periodically and diluted with DMF into a 10 mL volumetric flask. Emission spectra of the aliquot-DMF solutions were recorded between 500 to 650 nm at $\lambda_{\text{ex}} = 483$ nm. With the use of a calibration curve, the mass of DOX in the dialysis bag was calculated from the emission intensity at 592 nm. The weight of DOX loaded into the micelles was determined once the concentration of DOX in the dialysis bag no longer decreased with time. Finally, the polymer solutions were diluted to *ca.* 0.2 mg/mL with deionized water and stored at 4°C in the absence of light for subsequent *in vitro* drug-release and cytotoxicity experiments.

Drug Loading Efficiency (DLE) and Drug Loading Content (DLC) were as follows:

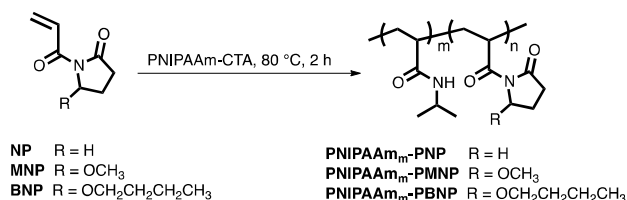
$$\text{DLE}(\%) = \frac{\text{mass of loaded DOX}}{\text{mass of DOX in the feed}} \times 100\%$$

$$\text{DLC}(\%) = \frac{\text{mass of loaded DOX}}{\text{mass of DOX-loaded micelles}} \times 100\%$$

Drug Release at 20°C and 37°C. A 50 mL volumetric flask was charged with 5 mL of DOX-loaded micelle solution (polymer concentration, 0.2 mg/mL) and diluted with phosphate buffered saline (PBS) solution (0.01 M, pH = 7.4). The content of this flask was distributed equally into ten vials (*i.e.*, 5 mL/vial, polymer concentration, 0.02 mg/mL) and placed in a single water bath at 20°C or 37°C. Over the course of several hours, a vial was removed periodically and placed in a centrifuge at *ca.* 4.4k rpm for 15 min. The supernatant was analyzed by DLS to ensure the absence of micelles. Emission spectra of the solutions (diluted in PBS) were recorded in the range of 500 to 650 nm at $\lambda_{\text{ex}} = 483$ nm. With the use of a calibration curve, the mass of DOX was calculated from the emission intensity at 592 nm.

In Vitro Cytotoxicity. *In vitro* cytotoxicity studies were conducted using the MCF-7 breast cancer cell line. MCF-7 cells were cultured in Dulbecco's modified Eagle's medium (DMEM) supplemented with 10% fetal bovine serum, 100 units/mL penicillin, 100 $\mu\text{g}/\text{mL}$ of streptomycin, and 0.25 $\mu\text{g}/\text{mL}$ of amphotericin B at 37°C and 5% CO_2 . Individual wells (96 well plates) were seeded with 5,000 cells/well and incubated for 24 hours prior to experimentation. To evaluate cytotoxicity, wells of MCF-7 cells were treated with 200 μL of free DOX solution, blank micelles, or DOX-loaded micelles (*ca.* 1-50 $\mu\text{g}/\text{mL}$) for 3 hours at either 20°C or 37°C. The cells were then washed free of DOX/micelle reagents with PBS and incubated at 37°C for an additional 48 hours. In experiments that evaluated cell viability as a function of DOX concentration (*i.e.* in the free form and loaded), formulations were incubated at 37°C for 72 h. Cells were then washed (3x) with PBS prior to

adding 100 μL of DMEM containing 10% AlamarBlue[®] reagent (used to quantitate cell survival by measuring reduction of non-fluorescent resazurin to fluorescent resorufin in metabolic active cells). After incubating at 37 $^{\circ}\text{C}$ for 3 hrs, fluorescence intensity was measured at 590 nm (excitation wavelength, 560 nm) using a microplate reader. Cell viability was expressed as a percentage by normalizing the fluorescence intensity of the experimental group relative to DMEM media treated cells; each experimental group was repeated in triplicate. Block copolymer concentrations were identical in all formulations used to compare cytotoxicity between DOX-loaded and blank micelles. For experiments that compared cytotoxicity between DOX-loaded micelles and free DOX, polymer concentrations were adjusted to ensure that DOX concentration (*ca.* 50 $\mu\text{g}/\text{mL}$) were identical in all formulations (since micelles were found to exhibit slightly different drug loadings based on core-structure).



Scheme 1 Synthesis of block copolymer hydrophobic segment.

Results and Discussion

Synthesis and Characterization of Block Copolymers

All thermoresponsive block copolymers were prepared according to Scheme 1. Macromolecular chain transfer agent PNIPAAm-CTA was synthesized via RAFT polymerization of *N*-isopropylacrylamide and used for all subsequent chain-extending polymerizations with the appropriate *N*-acryloyl-2-pyrrolidone monomer. Block copolymers with hydrophobic segments prepared from *N*-acryloyl-2-pyrrolidone (NP), *N*-acryloyl-5-methoxy-2-pyrrolidone (MNP), and *N*-acryloyl-5-butoxy-2-pyrrolidone (BNP) are designated as PNIPAAm-PNP, PNIPAAm-PMNP, and PNIPAAm-PBNP respectively. For each block copolymer type, two block copolymers that are distinguishable only by the length of the hydrophobic segment were prepared and are designated *short chain* or *long chain* throughout this article. All ¹H-NMR spectra (Fig. 2, S2-S7) exhibit resonances (*e.g.* α , β , ω , and κ , Fig. 2) and relative integral ratios that are consistent with those observed from homopolymer samples of each segment. The distinct chemical environment of the pyrrolidone hydrogen(s), ω , made it possible to estimate the degree of polymerization by comparing the integral ratio of $I_{\alpha} : I_{\omega}$. As such, the block copolymers were designated as PNIPAAm₇₂-PBNP₇₃, PNIPAAm₇₂-PBNP₂₆, PNIPAAm₇₂-PMNP₇₈, PNIPAAm₇₂-PMNP₂₉, PNIPAAm₇₂-PNP₇₉, and PNIPAAm₇₂-PNP₂₉. All GPC traces are predominantly monomodal with PDIs in the range of *ca.* 1.16–1.30, indicating that PNIPAAm-CTA initiation is efficient. As anticipated, reductions in retention times were observed in chromatograms for each block copolymer type upon extension of the pyrrolidone-based polymer block (Fig. 3, Fig. S9–S11), a phenomenon that is attributed to an increase in hydrodynamic volume as the length of the copolymer is extended.

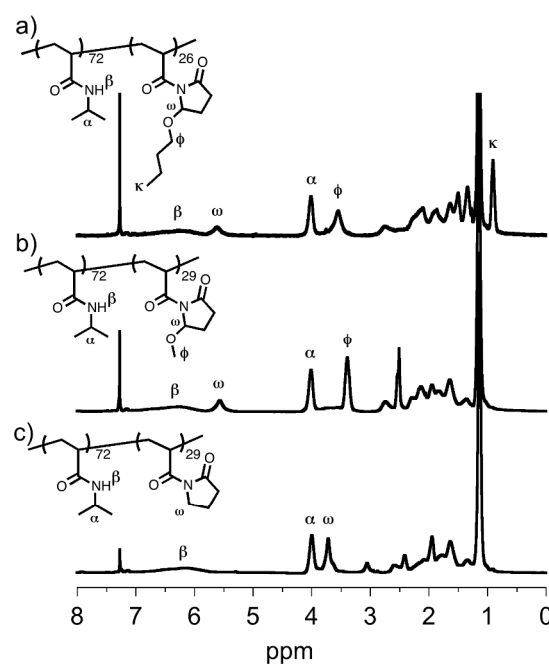


Fig. 2 ¹H NMR spectra (500 MHz, CDCl₃, 25 $^{\circ}\text{C}$) of a) PNIPAAm₇₂-PBNP₂₆, b) PNIPAAm₇₂-PMNP₂₉, and c) PNIPAAm₇₂-PNP₂₉.

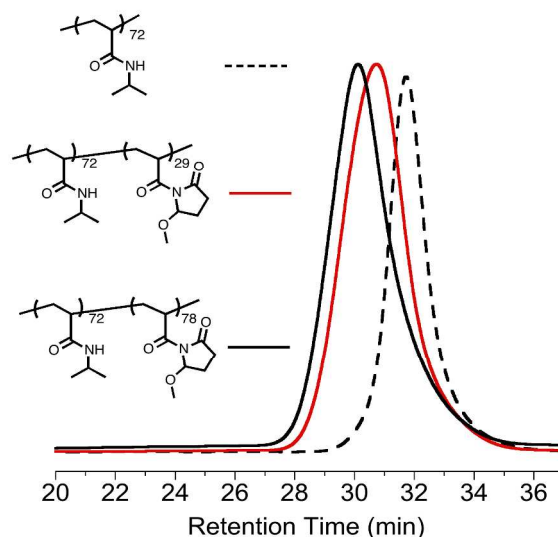


Fig. 3 GPC trace of a) PNIPAAm-CTA (black dashed), PNIPAAm₇₂-PMNP₂₉ (red-solid) and PNIPAAm₇₂-PMNP₇₈ (black solid). Relative to poly (methyl methacrylate) in DMF/0.01M LiBr.

Effect of Hydrophobic Block Structure on Critical Micelle Concentration and Micelle Size

Block copolymer self-assembly was detected by fluorescence spectroscopy using pyrene as a hydrophobic probe. As micelles with PNIPAAm coronae and P(B,M)NP cores were assembled with increasing copolymer concentration, pyrene partitioned into the hydrophobic cores resulting in a red shift in its excitation spectrum (*ca.* 334 nm to 337 nm), a phenomenon that arises from its vibrational band structure that is highly sensitive to changes in microenvironment polarity.^{64,65}

As such, association behavior was monitored by measuring the pyrene intensity ratio I_{337}/I_{334} as a function of copolymer concentration in water. From the appropriate plot (Fig. 4), a CMC value was estimated as the point of intersection between two linear lines of regression.

Overall, the results of this study show a distinct correlation between CMC and hydrophobic block structure (Table 1). Among the short chain block copolymers (Table 1, entries 2, 4, and 6), CMC values were found to decrease in the order of PNIPAAm₇₂-PNP₂₉ (CMC *ca.* 121.2 mg/L), PNIPAAm₇₂-PMNP₂₉ (CMC *ca.* 5.1 mg/L), and PNIPAAm₇₂-PBNP₂₆ (CMC *ca.* 1.2 mg/L). This trend is also observed among the long chain block copolymers where CMC values are reduced by an order of magnitude upon both the addition *and* lengthening of the alkoxy residue (Table 1, entries 1, 3, and 5, Fig. S12), indicating that only minor modifications to the pyrrolidone scaffold are required to significantly enhance the hydrophobic character of the polymer segment. Indeed, the CMC values for the alkoxy-bearing block copolymers are indicative of excellent micellar stability at low polymer concentrations, a property that is attractive for drug-delivery vehicles that are diluted upon entering the body's bloodstream.

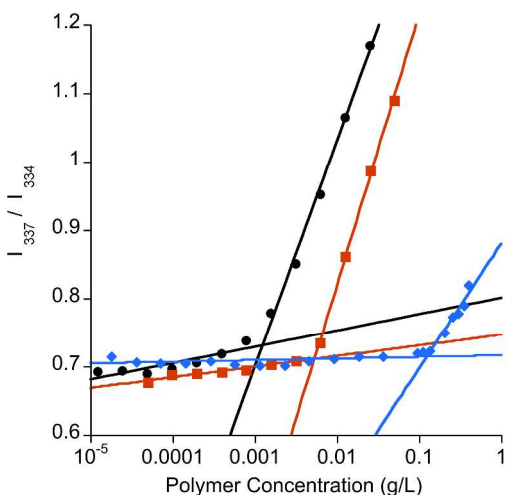


Fig. 4 The intensity ratio I_{337}/I_{334} obtained from pyrene excitation spectra of block copolymer solutions vs block copolymer concentration. PNIPAAm₇₂-PNP₂₉ (-◆-), PNIPAAm₇₂-PMNP₂₉ (-■-), and PNIPAAm₇₂-PBNP₂₆ (-●-).

Micelles were prepared by dialyzing block copolymer/DMF solutions (*ca.* 0.2 mg/mL) against deionized water. TEM of PNIPAAm₇₂-PBNP₂₆ (Fig. 5) confirmed the formation of regular spherical micelles with an average diameter of *ca.* 50 nm, a value in line with its number-averaged hydrodynamic diameter, D_h , determined by DLS (*ca.* 52.3 nm, Table 1, entry 2). Size differences among the short chain block copolymer micelles were found to be significant ($p < 0.05$, one way ANOVA), decreasing in the order of PNIPAAm₇₂-PNP₂₉, PNIPAAm₇₂-PMNP₂₉ and PNIPAAm₇₂-PBNP₂₆ (*ca.* 119.6 nm, 67.4 nm and 52.3 nm respectively). Based on CMC data, the trend may be attributed to the enhanced hydrophobic character of the pyrrolidone-based polymer blocks upon addition and lengthening of the alkoxy-residues, a phenomenon that is expected to increase attractive hydrophobic interfacial forces at the hydrophobic/hydrophilic block interface resulting in micelles with smaller surface areas.⁶⁶ Interestingly, this trend is reversed among long chain block copolymers micelles where D_h decreases in the order of PNIPAAm₇₂-PBNP₇₃,

PNIPAAm₇₂-PMNP₇₈, and PNIPAAm₇₂-PNP₇₉ (Table 1, entries 1, 3, and 5, $p < 0.05$, one way ANOVA, $n = 3$). While the origin of this trend is not understood at this time, the results suggest that the influence of the pyrrolidone residue on micelle size is block-length dependent. Nonetheless, the micelles prepared here are assembled into a size range (*ca.* 10-200 nm) that is optimal for nanoparticle drug carriers where long residence times in the blood are required for enhanced drug delivery.^{9,67}

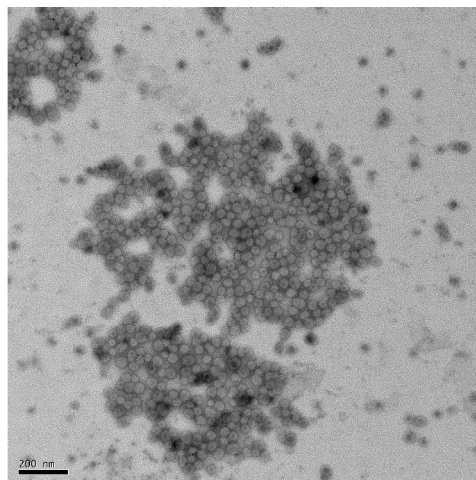


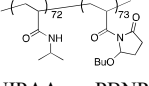
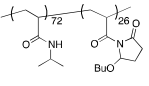
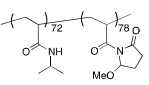
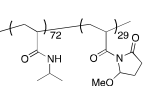
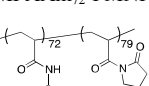
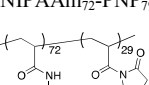
Fig. 5 TEM micrograph of PNIPAAm₇₂-PBNP₂₆ micelles negatively stained with uranyl acetate staining.

Thermal-induced Deformation and Aggregation

The thermoresponsive behaviour of our block copolymer micelles was investigated by turbidimetry and DLS. Micellar LCSTs (defined here as the temperature producing a 50% decrease in optical transmittance) in deionized water were measured to be in the range of *ca.* 33 to 41°C (Table 1), values that are slightly higher than those obtained from PBS solutions (Table S2) which we surmise is due to salting-out effects. Among the set of short chain block copolymers, micelles prepared from PNIPAAm₇₂-PNP₂₉ and PNIPAAm₇₂-PMNP₂₉ undergo significant thermal-induced aggregation upon exceeding their LCST as made evident by the large reductions in optical transmittance as more efficient light scatterers are formed (Fig. 6a, colored, y1-axis). This phenomenon was confirmed by variable-temperature DLS where particle sizes (Fig. 6b and c) increase significantly over the temperature range of 25 to 50°C.

In contrast, changes in D_h (Fig. 6d) are much less pronounced when micellar solutions prepared from PNIPAAm₇₂-PBNP₂₆ are heated above the LCST giving rise to a small reduction in optical transmittance (Fig. 6a, black, y2-axis), a trend that is also consistent with data collected from the long chain block copolymers (Fig. S14). Indeed, when taken together with both the CMC and DLS data presented in Table 1, these data indicate that the physicochemical properties of our micelles are highly sensitive to modest differences in hydrophobic pyrrolidone-based polymer structure, a feature that may have implications for establishing design criteria for highly efficient nano-scale delivery vehicles that do not require excessive adjustments to macromolecular scaffold

Table 1. Characterization data of thermoresponsive block copolymers.

| entry | copolymer | M_n^{NMR} | PDI ^a | D_h^b (nm) | CMC (mg/L) | LCST ^c (°C) | DLE ^d (%) | DLC ^e (%) | Release ^f 37°C (%) | Release ^f <20°C (%) |
|-------|--|-------------|------------------|--------------|------------|------------------------|----------------------|----------------------|-------------------------------|--------------------------------|
| 1 |  PNIPAAm ₇₂ -PBNP ₇₃ | 24000 | 1.20 | 91.5±3.0 | 0.4 | 37.0±1.7 | 82.4±1.9 | 28.7±2.1 | 22.7±2.0 | 4.7±1.2 |
| 2 |  PNIPAAm ₇₂ -PBNP ₂₆ | 14000 | 1.27 | 52.3±1.3 | 1.2 | 41.3±0.6 | 74.9±3.2 | 25.9±2.0 | 24.9±0.2 | 6.0±0.4 |
| 3 |  PNIPAAm ₇₂ -PMNP ₇₈ | 22000 | 1.30 | 85.9±2.7 | 2.6 | 38.7±0.6 | 72.4±2.7 | 25.3±1.5 | 25.2±1.0 | 6.5±0.6 |
| 4 |  PNIPAAm ₇₂ -PMNP ₂₉ | 13000 | 1.20 | 67.4±2.0 | 5.1 | 38.3±1.5 | 65.9±2.3 | 24.1±1.7 | 31.1±1.4 | 5.4±0.6 |
| 5 |  PNIPAAm ₇₂ -PNP ₇₉ | 19000 | 1.21 | 67.0±11.7 | 20.7 | 32.7±1.2 | 60.6±7.5 | 21.5±3.6 | 33.1±0.8 | 4.8±0.3 |
| 6 |  PNIPAAm ₇₂ -PNP ₂₉ | 12000 | 1.16 | 119.6±3.1 | 121.2 | 32.6±0.6 | 56.8±5.7 | 20.4±3.4 | 39.9±3.1 | 5.7±0.2 |

^a Determined by GPC (relative to poly(methyl methacrylate)) in 0.01M LiBr in DMF. ^b Determined by DLS. Values are expressed as a mean (number(%)) with standard deviation (n = 3). Sample preparation: [polymer] = 0.1 mg/mL. ^c Values are expressed as a mean with standard deviation (n = 3). ^d Drug loading efficiency (DLE) is defined as the mass ratio of loaded drug to drug in the feed solution. Values are expressed as a mean with standard deviation (n = 3). ^e Drug loading content (DLC) is defined as the mass ratio of the loaded drug to drug-loaded micelle. Values are expressed as a mean with standard deviation (n = 3). ^f Values are expressed as a mean with standard deviation (n = 3).

in order to improve drug carrier performance.

DOX Loading and Cumulative Thermoresponsive Release

DOX-loaded micelles were prepared by dialyzing an *N*-ethylacetamide solution of block copolymer, DOX-HCl, and triethylamine against deionized water under sink conditions. The use of *N*-ethylacetamide was critical to micelle formation as initial attempts using DMF or dimethylsulfoxide resulted in precipitation during dialysis. The hydrodynamic diameters of the drug-loaded micelles were measured by DLS and found to be shorter compared to their drug-free analogs (Tables S3 and S4) suggesting that intermolecular interactions between the drug and pyrrolidone-based polymer block are strong resulting in the formation of dense micellar coronae upon self-assembly. Drug loading efficiencies were determined using spectroscopic methods and found to increase in the order of PNIPAAm₇₂-PNP₂₉, PNIPAAm₇₂-PMNP₂₉, and PNIPAAm₇₂-PBNP₂₆ (*ca.* 57, 66, and 75% respectively, Table 1, entries 6, 4, and 2), differences that are significant ($p < 0.05$, one way ANOVA, n = 3) and attributed to enhanced cohesive forces (*i.e.*, London dispersion forces) between hydrophobic drug and core as the latter adopts more hydrophobic character. This trend was also observed among micelles prepared from PNIPAAm₇₂-PNP₇₉,

PNIPAAm₇₂-PMNP₇₈, and PNIPAAm₇₂-PBNP₇₃ where DOX encapsulation is greater than their respective short chain analogs. Moreover, drug loading contents (DLCs) were calculated to be in the range of *ca.* 20-29% (wt/wt) indicating high payload capacities and efficient drug encapsulation among these systems.

Time-dependent cumulative DOX release by the short-chain DOX-loaded micelles in PBS solution was evaluated at *ca.* 37°C and 20°C and the results illustrated in Fig. 7. In all cases, the extent of DOX release was suppressed at 20°C and enhanced at 37°C, reaching a plateau after *ca.* 10 h. Indeed, the results of this study are consistent with other works that report an enhanced rate of drug release from thermoresponsive amphiphilic block copolymer micelles at elevated temperatures,^{22,24,44} a phenomenon that has been postulated to arise from thinner micellar coronae and hydrophobic core deformation that can lead to enhanced drug release.⁶⁸ Interestingly, the overall percentage of drug release decreased significantly ($p < 0.05$, one way ANOVA) in the order of PNIPAAm₇₂-PNP₂₉, PNIPAAm₇₂-PMNP₂₉, and PNIPAAm₇₂-PBNP₂₆ (*ca.*, 40, 31, and 25% respectively, Table 1, entries 6, 4, and 2) despite the increasing order of DLE among these systems. This trend was also observed in studies employing long chain block copolymers (Table 1, entries 5, 3, 1, Fig. S42,

$p < 0.05$, one way ANOVA) and suggests that the mechanisms responsible for improving drug loading efficiency may also prevent efficient release upon thermal activation.

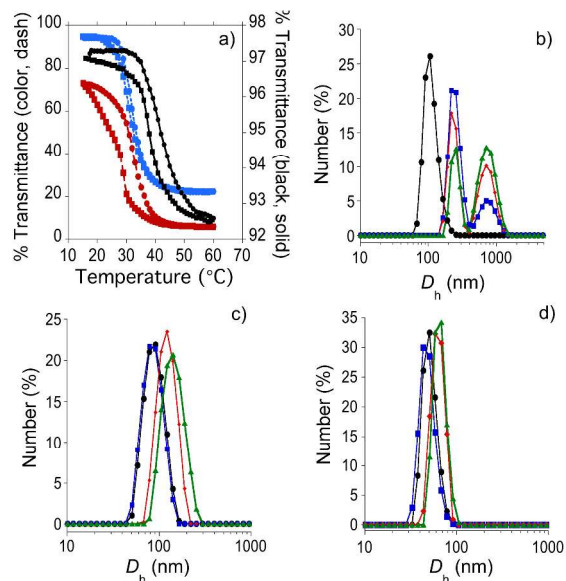


Fig. 6 a) LCST profiles for PNIPAAm₇₂-PNP₂₉ (blue circle, dash, forward scan, blue square, dash, reverse scan), PNIPAAm₇₂-PMNP₂₉ (red circle, dash, forward scan, red square dash, reverse scan), and PNIPAAm₇₂-PBNP₂₆ (black circle, solid, forward scan, black square, solid, reverse scan) micellar solutions determined by transmittance at 500 nm, [polymer] = 0.2 mg/mL. Size distribution of b) PNIPAAm₇₂-PNP₂₉ at ca. 25 °C (●), 35 °C (■), 40 °C (◆), and 50 °C (▲), c) PNIPAAm₇₂-PMNP₂₉ at ca. 25 °C (●), 35 °C (■), 40 °C (◆), and 50 °C (▲), and PNIPAAm₇₂-PBNP₂₆ at ca. 25 °C (●), 35 °C (■), 40 °C (◆), and 50 °C (▲).

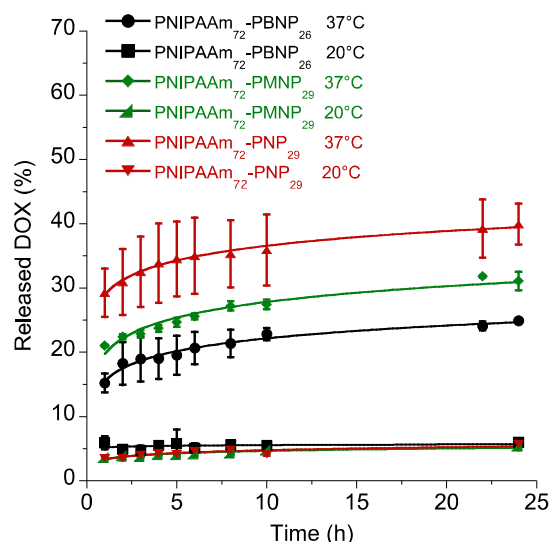


Fig. 7 DOX release from a) PNIPAAm₇₂-PNP₂₉ at 37 °C (▲) and 20 °C (▼), PNIPAAm₇₂-PMNP₂₉ at 37 °C (◆) and 20 °C (▲), and PNIPAAm₇₂-PBNP₂₆ 37 °C (●) and 20 °C (■). Data points are plotted as a mean with standard deviation ($n = 3$).

In vitro Cytotoxicity

DOX-loaded drug carriers have been shown to exhibit anti-cancer activity on a number of types of cancer cells and tumors.^{26,69,70,71,72} On the basis of these reports, the cytotoxic activity of our DOX-loaded micelles ([DOX], ca. 50 $\mu\text{g/mL}$) was evaluated *in vitro* against both free DOX ([DOX], ca. 50 $\mu\text{g/mL}$) and blank micelles (*i.e.* drug-free) at ca. 20 °C and 37 °C. MCF-7 breast cancer cells were incubated with the exogenous substrates for 3 h at the appropriate temperature then washed and evaluated for viability after 48 h. The results of this investigation show that at 37 °C, the cytotoxic activity in DOX-loaded micelle formulations is significantly greater ($p < 0.05$, Student's *t*-test) than their blank micellar controls adjusted for polymer concentration. Taken together with the observation that DOX-loaded micelles are less cytotoxic than DOX in its free form, the results are indicative of a sustained and incomplete drug release process during cell incubation that is consistent with the thermoresponsive release data illustrated in Fig. 7. Moreover, all DOX-loaded micelles exhibit a significantly higher cytotoxicity ($p < 0.05$, Student's *t*-test) in formulations incubated at 37 °C compared to 20 °C, a trend also observed in formulations containing free DOX and blank micelles indicating that differences in cell viability measured above and below the LCST cannot solely be attributed to thermoresponsive drug release.

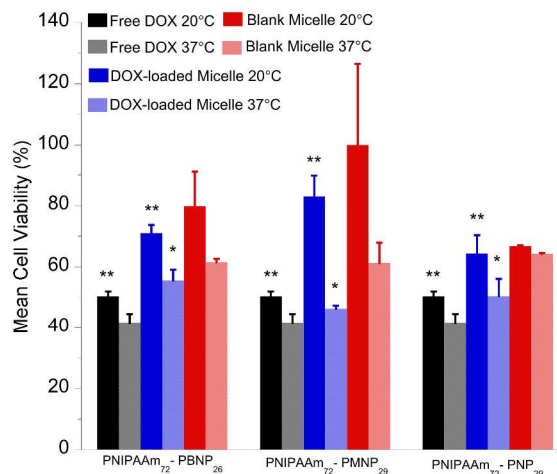


Fig. 8 In vitro cytotoxicity of blank micelles, free DOX, and DOX-loaded micelles at 20 and 37 °C. [DOX] \approx 50 $\mu\text{g/mL}$. [polymer] \approx 0.13-0.15 mg/mL. MCF-7 cells were incubated with the exogenous substrates for ca. 3 h, washed, and measured for viability after 48 h. Data are expressed in mean cell viability (%) with error bars indicating standard deviation. $n = 3$. * indicates that differences in mean cell viability between DOX-loaded and blank micelles at 37 °C are statistically significant ($p < 0.05$, Student's *t*-test). ** indicates that differences in mean cell viability between free DOX/DOX-loaded micelles at 20 °C and 37 °C are statistically significant ($p < 0.05$, Student's *t*-test).

Since the presence of both DOX and block copolymer appear to contribute to the overall cytotoxic activity of DOX-loaded micelles in formulations where [DOX] is ca. 50 $\mu\text{g/mL}$ and [polymer] is ca. 0.13-0.15 mg/mL (Fig. 8), a second investigation was conducted to evaluate the cytotoxicity of DOX-loaded micelles as a function of DOX concentration. In this study, MCF-7 breast cancer cells were incubated for 72 h at 37 °C to ensure that cells were exposed to the maximum amount

of drug released from the loaded micelles. Experiments were then repeated with both free DOX and blank micellar controls that were adjusted for drug and polymer concentration respectively. Indeed, the results of this investigation show that all DOX-loaded micelles exhibit cytotoxic activity that is comparable to free DOX in the concentration range of *ca.* 10 – 40 $\mu\text{g/mL}$ (Fig. 9), thus confirming their ability to serve as a drug carrier under *in vitro* conditions. Perhaps most importantly, the DOX-loaded micelles show enhanced cytotoxicity compared to blank micelle controls that are virtually nontoxic indicating the cell death likely arises from DOX and not the micelle itself.

Summary and Conclusions

A novel series of thermoresponsive block copolymer micelles with identical hydrophilic PNIPAAm corona and distinguishable poly(*N*-acryloylpyrrolidone) cores were examined to identify how minor adjustments to core-segment structure affect both micellar physicochemical properties and drug delivery performance among these systems. The results of our findings show that the addition of a single methoxy residue to the pyrrolidone scaffold can increase the overall hydrophobic character of the pyrrolidone-based polymer block, a result that is enhanced further by employing butoxy residues in their place. These modifications were also found to affect block copolymer self-assembly and intermicellar aggregation below and above the LCST respectively. Using DOX as a therapeutic hydrophobic payload, drug loading efficiencies were found to increase significantly in the order of PNIPAAm-PNP, PNIPAAm-PMNP, and PNIPAAm-PBNP indicating that drug encapsulation can be improved with only modest adjustments to macromolecular structure. Time-dependent drug release studies revealed that cumulative DOX release is significantly greater when the drug-loaded micelles are heated above the LCST, confirming the thermoresponsivity of these systems. Moreover, the cumulative release was found to decrease in the order of PNIPAAm-PNP, PNIPAAm-PMNP, and PNIPAAm-PBNP suggesting that the mechanisms responsible for improving encapsulation also impede efficient release. Indeed, this phenomenon presents a conundrum that warrants further investigation if thermoresponsive micelles with high loading capacities and efficient release profiles are to be realized. Finally, all blank micelles were found to exhibit cytotoxic activity at relatively high concentrations, however, formulations could be adjusted such that only DOX-loaded micelles express selectively high *in vitro* cytotoxicity upon heating through the micellar LCST. On the basis of the results reported here, future efforts will focus on preparing block copolymers with more structurally and electronically diverse pyrrolidone residues as a means to establishing a more comprehensive understanding of the structure/property/performance correlations that govern these systems, knowledge that we envision will ultimately lead to the realization of micelles that exhibit comparable drug loading efficiencies with significantly improved thermoresponsive release profiles.

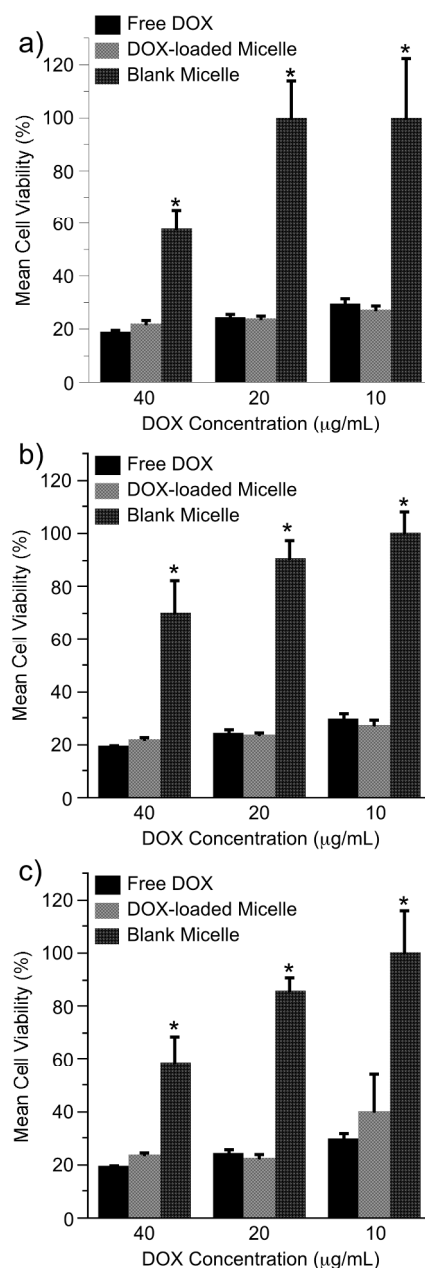


Fig. 9 In vitro cytotoxicity of DOX-loaded micelles prepared from a) PNIPAAm₇₂-PBNP₂₆, b) PNIPAAm₇₂-PMNP₂₉, and c) PNIPAAm₇₂-PNP₂₉. Data obtained from formulations of free DOX and blank micelles adjusted for polymer concentration are plotted for comparison. MCF-7 cells were incubated with the exogenous substrates for *ca.* 72 h at 37 °C. Data are expressed in mean viability (%), and error bars indicate standard deviation. $n=3$. * indicates that differences in mean cell viability between DOX-loaded micelle and blank micelle formulations are statistically significant ($p < 0.05$, Student's *t*-test).

Acknowledgements

The authors thank Rutgers University for financial support for this work.

Notes and references

^a Department of Chemistry, Rutgers University-Newark, 73 Warren Street, Newark, New Jersey 07102, United States..

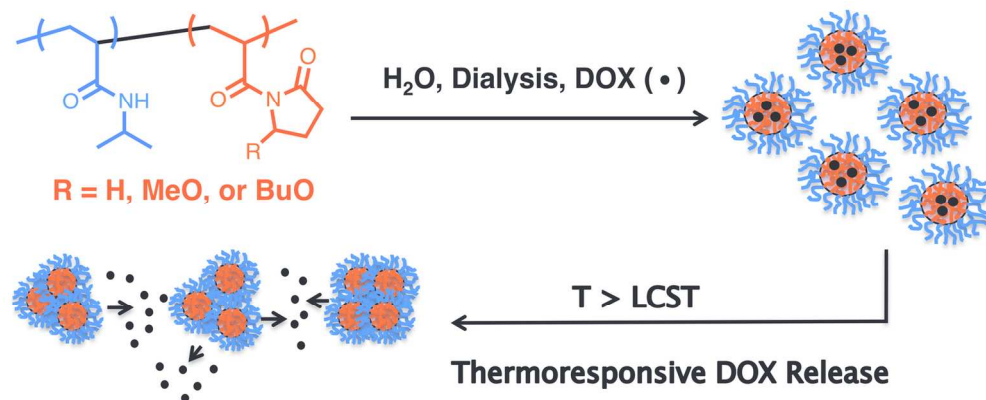
^b Department of Pharmaceutics, Ernest Mario School of Pharmacy, Rutgers University, 160 Frelinghuysen Road, Piscataway, New Jersey 08854-8022, United States.

^c Department of Biological Sciences, Rutgers University-Newark, 195 University Avenue, Newark, New Jersey 07102, United States.

† Electronic Supplementary Information (ESI) available: Additional characterization and experimental data. See DOI: 10.1039/b000000x/

- ¹ R. Gref, Y. Minamitake, M. T. Peracchia, V. Trubetsky, V. Torchilin and R. Langer, *Science* 1994, **263**, 1600-1603.
- ² K. Kataoka, A. Harada and Y. Nagasaki, *Adv. Drug Delivery Rev.* 2001, **47**, 113-131.
- ³ N. Rapoport, A. Marin, Y. Luo, G. D. Prestwich, M. D. and Muniruzzaman, *J. Pharm. Sci.* 2002, **91**, 157-170.
- ⁴ In *Amphiphilic Block Copolymers: Self Assembly and Applications*; P. Alexandridis and B. Lindman, Eds.; Elsevier Science: Amsterdam, 2000. pp. 347-377.
- ⁵ N. Rapoport, *Colloids and Surfaces, B: Biointerfaces* 1999, **16**, 93-111.
- ⁶ A. Marin, M. Muniruzzaman and N. Rapoport, *J. Controlled Release*, 2001, **71**, 239-249.
- ⁷ A. Marin, M. Muniruzzaman and N. Rapoport, *J. Controlled Release*, 2001, **75**, 69-81.
- ⁸ J. H. Lee, H. B. Lee and J. D. Andrade, *Prog. Poly. Sci.* 1995, **20**, 1043-1079.
- ⁹ D. M. McDonald and P. Baluk, *Cancer Res.* 2002, **62**, 5381-5386.
- ¹⁰ G. S. Kwon and K. Kataoka, *Adv. Drug. Deliv. Rev.* 1995, **16**, 295-309.
- ¹¹ H. M. Aliabadi and A. Lavasanifar, *Expert Opin. Drug Deliv.* 2006, **3**, 139-162.
- ¹² M. Ferrari, *Nat. Rev. Cancer*, 2005, **5**, 161-171.
- ¹³ H. Maeda, L. M. Seymour and Y. Miyamoto, *Bioconjugate Chem.* 1992, **3**, 351-362.
- ¹⁴ K. S. Soppimath, D. C. W. Tan and Y. Y. Yang, *Adv. Mater.* 2005, **17**, 318-320.
- ¹⁵ E. S. Lee, H. J. Shin, K. Na and Y. H. Bae, *J. Controlled Release*, 2003, **90**, 363-374.
- ¹⁶ E. S. Lee, K. Na and Y. H. Bae, *Nano Lett.* 2005, **5**, 325-329.
- ¹⁷ B. S. Kim, J. M. Qiu, J. P. Wang and T. A. Taton, *Nano Lett.* 2005, **5**, 1987-1991.
- ¹⁸ J. H. Park, G. von Maltzahn, E. Ruoslahti, S. N. Bhatia and M. J. Sailor, *Angew. Chem. Int. Ed.* 2008, **47**, 7284-7288.
- ¹⁹ S. Cammas, K. Suzuki, C. Sone, Y. Sakurai, K. Kataoka and T. Okano, *J. Controlled Release*, 1997, **48**, 157-164.
- ²⁰ H. Wei, X. Z. Zhang, Y. Zhou, S. X. Cheng and R. X. Zhou, *Biomaterials* 2006, **27**, 2028-2034.
- ²¹ M. A. Ward and T. K. Georgiou, *Polymers* 2011, **3**, 1215-1242.
- ²² M. Nakayama, T. Okano, T. Miyazaki, F. Kohori, K. Sakai and M. Yokoyama, *J. Controlled Release*, 2006, **115**, 46-56.
- ²³ M. Heskins and J. E. Guillet, *J. Macromol. Sci. Chem. A2*, 1968, 1441-1455.
- ²⁴ J. E. Chung, M. Yokoyama, M. Yamato, T. Aoyagi, Y. Sakurai and T. Okano, *J. Controlled Release*, **1999**, **62**, 115-127.
- ²⁵ F. Kohori, K. Sakai, T. Aoyagi, M. Yokoyama, M. Yamato, Y. Sakurai and T. Okano, *Colloids Surf B: Biointerfaces*, 1999, **16**, 195-205.
- ²⁶ S. Q. Liu, Y. W. Tong and Y. Y. Wang, *Biomaterials* 2005, **26**, 5064-5074.
- ²⁷ S. Q. Liu, N. Wiradharma, S. J. Gao, S. Y. W. Tong and Y. Y. Yang, *Biomaterials* 2007, **28**, 1423-1433.
- ²⁸ H. Wei, C. Cheng, C. Chang, W. Q. Chen, S. X. Cheng, X. Z. Zhang and R. X. Zhou, *Langmuir* 2008, **24**, 4564-4570.
- ²⁹ H. Wei, X. Z. Zhang, H. Cheng, W. Q. Chen, S. X. Chen and R. X. Zhuo, *J. Controlled Release*, 2006, **116**, 266-274.
- ³⁰ Y. Y. Li, X. Z. Zhang, H. Cheng, J. L. Zhu, U. N. Li, S. X. Cheng and R. X. Zhuo, *Nanotechnology* 2007, **18**, 505101-505108.
- ³¹ Y. Y. Li, X. Z. Zhang, H. Cheng, J. L. Zhu, S. X. Cheng and R. X. Zhuo, *Macromol. Rapid Commun.* 2006, **27**, 1913-1919.
- ³² C. Cheng, H. Wei, X. Z. Zhang, S. X. Cheng, and R. X. Zhuo, *J. Biomed. Mater. Res. A* **2009**, **88A**, 814-822.
- ³³ W. Q. Chen, H. Wei, S. L. Li, J. N. Feng, J. Nie, X. Z. Zhang and R. X. Zhuo, *Polymer* 2008, **49**, 3965-3972.
- ³⁴ C. Cheng, H. Wei, J. L. Zhu, C. Chang, H. Cheng, C. Li, S. X. Cheng, X. Z. Zhang, and R. X. Zhuo, *Bioconjugate Chem.* 2008, **19**, 1194-1201.

- ³⁵ D. Attwood, C. Booth, S. G. Yeates, C. Chaibundit and N. Ricardo, *Int. J. Pharm.* 2007, **345**, 35-41.
- ³⁶ S. W. Kim, Y. Z. Shi, J. Y. Kim, K. N. Park and J. X. Cheng, *Expert Opin. Drug. Deliv.* 2010, **7**, 49-62.
- ³⁷ K. Letchford, R. Liggins and H. Burt, *J. Pharm. Sci.* 2008, **97**, 1179-1190.
- ³⁸ J. B. Liu, Y. H. Xiao and C. Allen, *J. Pharm. Sci.* 2004, **93**, 132-143.
- ³⁹ Y. X. Zhu, L. Che, H. M. He, Y. Jia, J. X. Zhang and X. H. Li, *J. Controlled Release* 2011, **152**, 317-324.
- ⁴⁰ G. Y. Li, S. Song, L. Guo and S. M. Ma, *J. Polym. Sci., Part A; Polym. Chem.* 2008, **46**, 5028-5035.
- ⁴¹ K. M. Huh, H. S. Min, S. C. Lee, H. J. Lee, S. Kim and K. Park, *J. Controlled Release*, 2008, **126**, 122-129.
- ⁴² K. M. Huh, S. C. Y. W. Cho, J. Lee, J. H. Jeong and K. Park, *J. Controlled Release*, 2005, **101**, 59-68.
- ⁴³ L. L. Chang, L. D. Deng, W. W. Wang, Z. S. Lv, F. Q. Hu, A. J. Dong and J. H. Zhang, *Biomacromolecules* 2012, **13**, 3301-3310.
- ⁴⁴ J. E. Chung, M. Yokoyama and T. Okano, *J. Controlled Release*, 2000, **65**, 93-103.
- ⁴⁵ F. Haaf, A. Sanner and F. Straub, *Polym. J.* 1985, **17**, 143-152.
- ⁴⁶ A. J. M. D'Souza, R. L. Schowen and E. M. Topp, *J. Controlled Release* 2004, **94**, 91-100.
- ⁴⁷ F. Fisher and S. Bauer, *Chem. Unserer Zeit*, 2009, **43**, 376-383.
- ⁴⁸ R. Bhat and A. Pietrangelo, *Macromol. Rapid. Commun.* 2013, **32**, 447-451.
- ⁴⁹ H. J. Lai, G. T. Chen, P. Y. Wu and Z. C. Li, *Soft Matter* 2012, **8**, 2662-2670.
- ⁵⁰ N. Yan, J. Q. Zhang, Y. Yuan, G. T. Chen, P. J. Dyson, Z. C. Li and Y. Kou, *Chem. Commun.* 2010, 1631-1633.
- ⁵¹ G. T. Chen, C. H. Wang, J. G. Zhang, Y. Wang, R. Zhang, F. S. Du, N. Yan, Y. Kou and Z. C. Li, *Macromolecules* 2010, **43**, 9972-9981.
- ⁵² J. Sun, Y. F. Peng, Y. Chen, Y. Liu, J. J. Deng, L. C. Lu and Y. Cai, *Macromolecules* 2010, **43**, 4041-4049.
- ⁵³ T. Trellenkamp and H. Ritter, *Macromolecules* 2010, **43**, 5538-5543.
- ⁵⁴ N. Yan, J. G. Zhang, Y. Y. Tong, S. Y. Yao, C. X. Xiao, Z. C. Li, and Y. Kou, *Chem. Commun.* 2009, 4423-4425.
- ⁵⁵ T. Trellenkamp and H. Ritter, *Macromol. Rapid Commun.* 2009, **30**, 1736-1740.
- ⁵⁶ J. J. Deng, Y. Shi, W. D. Jiang, Y. F. Peng, L. C. Lu and Y. L. Cai, *Macromolecules* 2008, **41**, 3007-3014.
- ⁵⁷ G. M. Iskander, L. E. Baker, D. E. Wiley and T. P. Davis, *Polymer* 1998, **39**, 4165-4169.
- ⁵⁸ R. L. Mompalmer, M. Karon, S. E. Siegel and F. Avila, *Cancer Res.* 1976, **36**, 2891-2895.
- ⁵⁹ Y. K. Chong, J. Krstina, T. P. T. Le, G. Moad, A. Postma, E. Rizzardo and S. H. Thang, *Macromolecules* 2003, **36**, 2256-2272.
- ⁶⁰ G. Moad, E. Rizzardo and S. H. Thang, *Polymer* 2008, 1079-1131.
- ⁶¹ C. A. Evans and S. J. Miller, *J. Am. Chem. Soc.* 2003, **125**, 12394-12395.
- ⁶² T. E. Horstmann and D. J. Guerin, *Angew. Chem. Int. Ed.* 2000, **39**, 3635-3638.
- ⁶³ I. Hevus, A. Modgil, J. Daniels, A. Kohut, C. W. Sun, S. Staflien and A. Voronov, *Biomacromolecules* 2012, **13**, 2537-2545.
- ⁶⁴ K. Kalyanasundaram, and J. K. Thomas *J. Am. Chem. Soc.* 1977, **99**, 2039-2044.
- ⁶⁵ D. C. Dong, M. A. Winnik, *Can. J. Chem.* 1984, **62**, 2560-2565.
- ⁶⁶ J. N. Isrealachvili, In *Intermolecular & Surface Forces: Second Edition*; Academic Press: London, 1991. pp 366-394.
- ⁶⁷ X. P. Duan and Y. P. Li, *Small* 2013, **9**, 1521-1532.
- ⁶⁸ X. Wan, T. Liu and S. Liu, *Biomacromolecules* 2011, **12**, 1146-1154.
- ⁶⁹ C. Y. Chen, T. E. Kim, W. C. Wu, C. M. Huang, C. W. Mount, Y. Tian, S. H. Jang, S. H. Pun, and A. K. Y. Jen, *Biomaterials* 2013, **34**, 4501-4509.
- ⁷⁰ N. V. Cuong, Y. L. Li and M. F. Hsieh, *J. Mater. Chem.* 2012, **22**, 1006-1020.
- ⁷¹ L. Battaglia, M. Gallarate, E. Peira, D. Chirio, E. Muntoni, E. Biasibetti, M. T. Capucchio, A. Valazza, P. P. Panciani, M. Lanotte, D. Schiffer, L. Annovazzi, V. Caldera, M. Mellai and C. Riganti, *J. Pharm. Sci.* 2014, **103**, 2157-2165.
- ⁷² T. Nakanishi, S. Fukushima, K. Okamoto, M. Suzuki, Y. Matsumura, M. Yokoyama, T. Okano, Y. Sakurai, and K. Kataoka, *J. Controlled Release*, **2001**, **74**, 295-302.



72x29mm (600 x 600 DPI)